Calibration and appliance of the Wilkins Damage Model for cast Aluminium

Christian Mühlstätter

LKR Leichtmetallkompetenzzentrum Ranshofen GmbH, Austrian Institute of Technology

1 Abstract

The application of Aluminium cast alloy in automotive fields faces increasing interest. The advantages of Aluminium cast alloys are being a well-established alloy in manufacturing processes, the function integrity and a relatively low weight. The presence of pores and further voids constitutes a specific material behaviour and establishes a challenge in modelling of cast material. Furthermore, the low ductility asks for advanced numerical models to predict structural failure. Therefor Finite Element (FE) Simulation tools, e. g. LS-Dyna, are used. The characteristic of these numerical software tools is the determination of strains and the corresponding stresses. The correlation between these mechanical parameters is achieved by the constitutive equation or material law.
The material behaviour of cast aluminium in FE-analysis is typically considered as elasto-plastic. In high deformation processes not only the constitutive behaviour has to be taken into account, but also material damage and failure need to be considered. Therefore, several damage and failure models exist, e.g. GISSMO and Gurson.
However, most of the available and implemented damage models are formulated by a high amount of phenomenological parameters. This results in flexibility and also in the necessity of deep knowledge in material modelling, for complex material testing and calibration of the model parameters.
The aim of this study is the investigation and validation of the material damage model ***MAT_PLASTICITY_WITH_DAMAGE_ORTHO(_RCDC)** or ***MAT_082**, introduced by Wilkins, for aluminium cast alloys.
A procedure for the calibration of this material damage model is introduced by different tension test specimens. Finally, a validation test is performed by a crushing load applied on a hat profile. The comparison of simulation with experiments exhibits a deviation of the absorbed energy of just 3 % related to experimental data.

2 Introduction

The material evolution and consideration of new materials is a key issue in light weight design. Materials with promising properties, e.g. low weight and productive manufacturing processes, are cast light metals. Modelling the behaviour of materials in numerical finite element models in general composes the constitution of a stress-strain relationship through material laws in combination with damage and failure criteria. The elasto-plastic material consideration leads to stress-strain data which allow for an evaluation of material damage. For upcoming materials, a strategy for material characterisation and the application of material models needs to be developed.
In contrast to wrought alloys, some additional challenges are related to cast alloys, e.g. the presence of pores and shrinkage defects. These voids may be involved in the mechanism of ductile fracture which is an accumulation of the micromechanical phenomena as void nucleation, void growth and coalescence.
The theory of material damage is based on micromechanical modelling of ductile fracture introduced by Gurson [1] and subsequent works of Tvergaard and Needleman [2]. The original approach of Gursen captures material damage caused by hydrostatic stress, but does not consider material failure in shear dominated load cases. The modification of the Gurson Model by Nahshon and Hutchinson [3] overcomes this weakness. Additional, phenomenological approaches for damage modelling of metallic materials are proposed, e.g. by Johnson and Cook [4]. These consider the influence of strain rate effects and temperature effects on the damage behaviour. A further approach is called Generalized Incremental Stress State dependent Damage Model (GISSMO) and is implemented in LS-Dyna [5]. The damage

consideration in GISSMO is assumed as function of plastic equivalent strain, stress triaxiality and the Lode Stress Parameter. Since GISSMO is developed for describing a wide range of different material behaviour, a high amount of phenomenological parameters has to be calibrated. Thus, a comprehensive knowledge of material modelling is necessary for the calibration of GISSMO.
An advanced Material Damage Model, introduced by Wilkins [6], is investigated in this paper. In this study, the Wilkins Damage Model is calibrated for an AlSi10 cast alloy by means of tensile test coupons with different geometries. A validation test is performed by application of hat profiles subjected to crushing load which proves the validity of the damage model and its applicability.

3 Damage modelling

Numerical simulations of Aluminium cast alloys without the consideration of material failure, as a result of material damage, leads to significant overestimated results. Since low ductility causes a limitation in high deformation processes, e.g. crash, the consideration of material damage is necessary in order to capture reasons for this material behaviour. Material failure is obtained as a cumulative parameter of material damage which results out of an evolution of micromechanical phenomena void nucleation, void growth and void coalescence. Hence, the damage behaviour until the onset of fracture needs to be investigated for the material of interest.
Essentially, numerical simulations determine stresses by the application of the constitutive material law and the derived strains. Several stress increment causes a corresponding damage increment which is accumulated over the simulation duration. Therefore, each stress state needs to be reduced to damage equivalent parameters. An actual stress state is fully described by the Lode stress parameter and the stress triaxiality [7]. The formulation of these parameters asks for theory of tensor formalism represented by the second and third invariant:

$$J_2 = \frac{1}{2}\boldsymbol{s}:\boldsymbol{s} \tag{1}$$

$$J_3 = \det \boldsymbol{s} \tag{2}$$

In equation 1 and 2, $\boldsymbol{s}$ denotes the deviatoric stress tensor. The deviatoric stress of an actual stress state leads to distortion in the material which after yield strength corresponds to the damage effect of void linkage. The Lode stress parameter μ_σ is used in several damage models, e.g. GISSMO. μ_σ covers the second and third deviatoric stress invariant and is introduced by Lode in 1927 in the form:

$$\mu_\sigma = \frac{3\sqrt{3}}{2}\frac{J_3}{J_2^{\frac{3}{2}}} \tag{3}$$

The influence of the complementary part to the deviatoric stress, the hydrostatic stress, is also considered in damage modelling. The hydrostatic stress is represented by the scalar σ_H and appears in equation 4 in the formulation of the stress triaxiality as

$$\eta = \frac{\sigma_H}{\sigma_{Mises}}, \tag{4}$$

where σ_{Mises} denotes the Von Mises equivalent stress. The stress triaxiality is considered as the crucial parameter for modelling of ductile damage. Hence, several damage models, e.g. Johnson-Cook, GISSMO, take the stress triaxiality into account.

4 Wilkins Damage Model in LS-Dyna

The Wilkins Damage Model is implemented in *LS-Dyna*, keyword ***MAT_082** or synonymous as ***MAT_PLASTICITY_WITH_DAMAGE_ORTHO(_RCDC).** This model uses an elasto-viscoplastic constitutive law and has an option for involving the Wilkins Damage Model or an alternative damage formulation which is purely based on plastic equivalent strain.

The approach of Wilkins [6] considers the actual stress state and the corresponding equivalent plastic strain $\varepsilon_{pl,equ}$. This information is taken into account by the damage evolution variable D as follows:

$$D = \int \omega_1 \, \omega_2 \, d\varepsilon_{pl,equ} \tag{5}$$

The parameters ω_1 and ω_2 contain the hydrostatic stress σ_H and the deviatoric principle stresses s_1, s_2 and s_3 as depicted in equation 6 and 7:

$$\omega_1 = \left(\frac{1}{1-\gamma \, \sigma_H}\right)^{\alpha} \tag{6}$$

and

$$\omega_2 = (2 - A_D)^{\beta}. \tag{7}$$

ω_1 and ω_2 denote the main characteristic of the approach of Wilkins which appears in a separated consideration of the hydrostatic stress σ_H and the deviatoric stresses s_1, s_2 and s_3 through A_D. The parameter A_D in Equation 7 is composed by the deviatoric principal stresses (equation 8) which obeys the condition $s_1 > s_2 > s_3$ with the operating range between [0,1]. Furthermore, phenomenological parameters, denoted as α, β and γ are included in Equation 6 and 7.

$$A_D = \max\left(\left|\frac{s_2}{s_3}\right|, \left|\frac{s_2}{s_1}\right|\right) \tag{8}$$

The Wilkins parameter A_D, depicted as black solid line in figure 1, shows an alternating behaviour in the range of [0, 1]. Figure 1 shows an investigation on the Wilkins parameter A_D and the Lode Stress Parameter μ_σ in plastic equivalent strain versus stress triaxiality representation. According to equation 7, increasing values of A_D lead to decreasing material damage. It is visible that the damage parameter A_D and hence ω_2 contributes significant to damage D in triaxiality regime $\eta = 0$ and also in biaxial tension, $\eta = 0.66$. Furthermore, the triaxilitiy regime of $\eta = -0.33$ exhibits an extrema of A_D whereas this triaxiality do not play a prominent role in damage occurrence [8]. This aspect has an impact on the calibration nature of the Wilkins Damage Model. It allows a quasi-separated consideration of shear or tension dominated loads with coupling effects in biaxial tension.

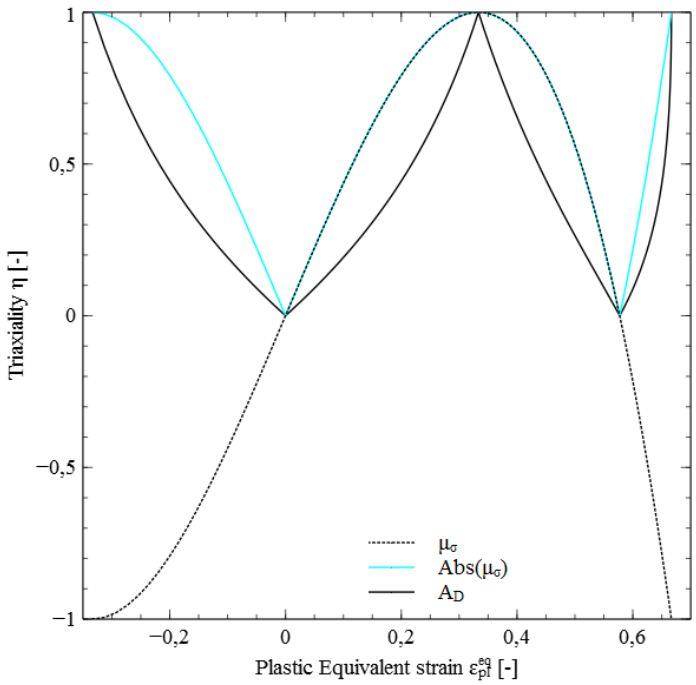

Fig. 1: Investigation on the Wilkins Parameter A_D compared to the Lode Stress Parameter μ_σ and the absolute amount of them

Furthermore, the absolute value of the Lode Stress Parameter is considered in figure 1. It is visible that the Wilkins Damage Parameter has the same extrema as the absolute value of the Lode Stress Parameter. As depicted in section 3, the Lode Stress Parameter is also formulated by the deviatoric stress part and plays a prominent role in failure modelling. The Lode Stress Parameter, black dotted line, appears as alternating parameter in the range of $[-1, 1]$. In conclusion of the investigation in figure 1, a Lode Parameter dependent characteristic, or precisely the absolute value of the Lode Parameter, of the Wilkins Damage Model is observed.
Previous equations 5, 6, 7 and 8 constitute the mathematical framework for the modelling of ductile damage. The accumulation of damage increments is conducted by equation 5. The description of material failure asks for additional examination of these data. The implementation in LS-Dyna consists of further equations, e.g. for the nonlocal formulation of material damage by the critical damage D_c,

$$D_c = D_0\left(1 + b\,|\nabla D|^{\lambda}\right). \tag{9}$$

In equation 9 ∇D denotes the spatial damage gradient and D_0, b and λ are phenomenological parameters. The nonlocal formulation is intended to reduce the mesh dependency of the damage model. The discretisation in FE simulation causes an approximation of the real geometry and subsequently of the deformation. A change in discretisation results in different precision of the deformation approximation. Material damage is initiated by local material deformations, e.g. necking. The caption of local deformations strongly depends on the discretisation. The nonlocal formulation in equation 9 constitutes an approach which is intended to cause less mesh sensitivity of the Wilkins Damage Model. Furthermore, the accumulated damage from equation 5 is applied for the criterion

$$\frac{D}{D_c} > 1, \tag{10}$$

which enables the material degradation in case the accumulated damage reaches the critical damage. Material degradation is a further history variable of ***MAT_082** and is formulated as

$$F = \frac{D - D_c}{D_s}. \tag{11}$$

The parameter D_s constitutes a further phenomenological parameter for the calibration of material degradation. Figure 2 shows two force versus displacement curves of a tension test simulation. The first curve (figure 2, black dotted) is a theoretical representation, because the simulation is set up with pure elasto-plastic material behaviour without damage. The black solid line in figure 2 shows a force versus displacement curve in application of ***MAT_082.** Furthermore, the history variables of material damage D and material degradation F is depicted in magenta and cyan representation. Force versus displacement data is defined globally for the tension test coupon. The history variables are element related parameters. Material damage steadily increases in tension test simulation and is accumulated until the criterion of equation 10 is fulfilled. Enabling material degradation leads to softening due to material damage in the force versus displacement behaviour and to an increasing history variable F. Material failure occurs at a specific value of F, depending on the calibration of the model. The gap in displacement between the separation of the force versus displacement curves and the onset of material degradation may be explained by the comparison of global and local, element related variables, i.e. the history variables define the behaviour of the element which fail last in simulation.

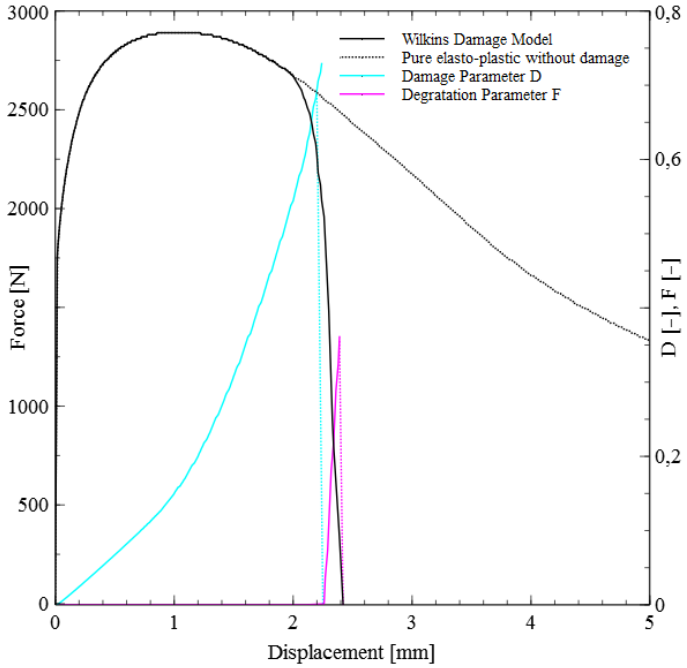

Fig. 2: Force versus displacement curve of a tension test simulation with and without the Wilkins Damage Model and the evolution of the history variables D and F for material damage and material degradation of ****MAT_082****.*

5 Material characterisation

As discussed in section 4, the Wilkins Damage Model demands several phenomenological parameter, namely α, β and γ for weighting of different stress parts, D_0, b and λ for the calibration of the nonlocal formulation and D_s for the calibration of the material degradation. In this study, the calibration of the material model is carried out by reverse engineering. This is a stringent approach to capture the behaviour for a phenomenological model description. For this purpose, the damage behaviour in different load cases has to be investigated. As previously argued, the mechanism of ductile damage is crucially influenced by stress triaxiality which constitutes the strategy of the damage behaviour characterisation in different triaxiality regimes. Figure 3 shows the geometries of the different tensile test coupons which are used in this study. The entire test series is performed on a tensile test rig which ensures low effort on tool configuration. Due to different geometries, several main triaxialitys occur in the middle section. The flat tensile geometry (figure 3, left) causes a triaxiality of $\eta = \frac{1}{3}$ under tensile load until necking occurs. The characterisation in laterally confined tension, triaxiality of $\eta = 0.57$, is carried out by the notched tensile geometry, depicted in figure 3, 2nd left. Furthermore, the $0°$ shear test and the Merklein specimen deliver data for the characterisation of a damage model in the triaxiality regime of $\eta = 0$. These four test geometries build a test setup for the positive triaxiality field of $\eta = 0$ to $\eta = 0.57$. Numerical simulations including material damage show that material failure essentially occurs in this triaxiality field [7]. Stress traxiality lower than $-\frac{1}{3}$ has no significance in damage modelling, because $\eta = -\frac{1}{3}$ represents a cut-off value for material failure [8]. Regarding the investigation in section 4, the approach of Wilkins considers two effects, hydrostatic stress and deviatoric stress, for ductile damage. Furthermore, the model shows a weak coupling of shear dominated and tension caused damage. Hence, the calibration of the damage model in triaxiality regime 0 is carried out by the Wilkins parameter β and γ by means of reverse engineering of the Merklein and shear geometry. In contrast, the tension triaxiality regime is calibrated by the Wilkins Parameter α and reverse engineering of the flat tensile and notched tension geometry. This procedure generates phenomenological sampling points and the remaining triaxiality regions are adjusted by means of the Damage formulation of Wilkins.

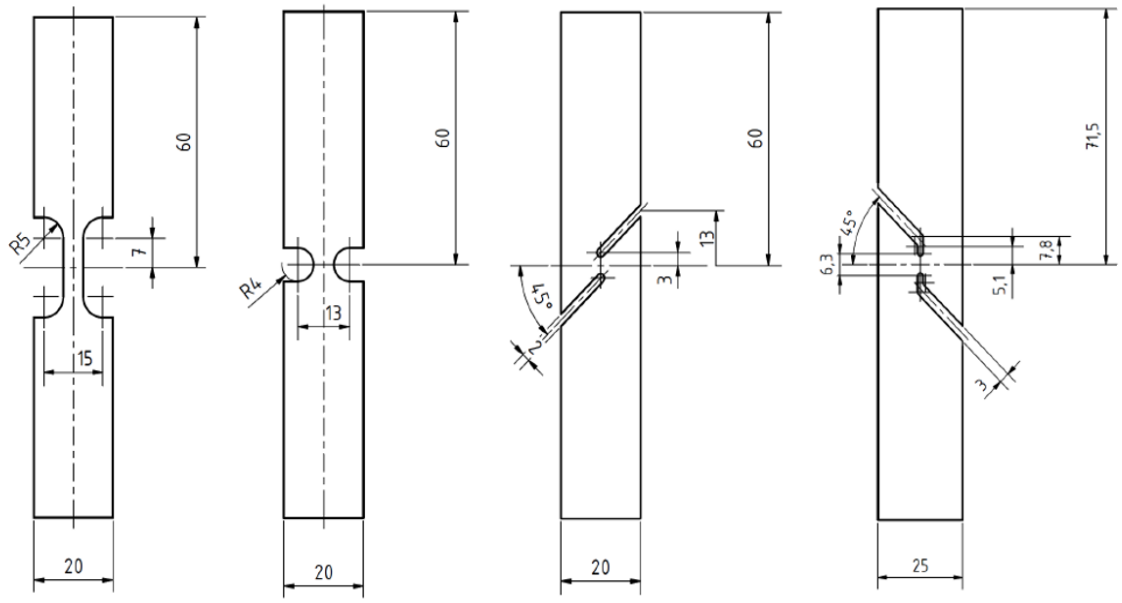

Fig. 3: Geometries of the tensile test coupons flat tensile (left), notched tensile (2nd left), 0° shear (2nd right) and Merklein (right), for the characterisation of the material damage behaviour.

To illustrate the characteristic of a damage model, the representation in plastic equivalent strain versus stress triaxiality is proposed. Figure 4 shows the load paths of the different test geometries in this representation. These load paths are extracted from FE simulations of the test coupons in application of the calibrated Wilkins Damage Model. For this purpose, the history of an element in the exposed, middle section of each geometry is considered until failure occurs. Obviously, the triaxiality varies during tensile test which is a distinct characteristic of ductile damage.

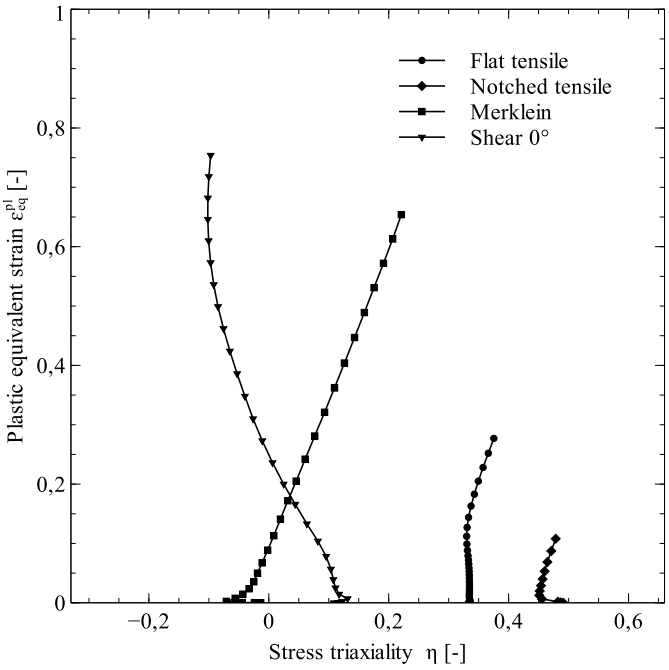

Fig. 4: Load paths of the tensile tests with different geometries in representation of plastic equivalent strain versus stress triaxiality

6 Simulation results and experimental validation

After calibration, the material model is applied on a crushing simulation of a hat profile. For validation purpose, an experimental crushing test is set up. The crushing velocity is $5\frac{mm}{s}$ and the maximum displacement is $100\,mm$. The experimental test is performed on an $1000\,kN$ ITC Interlaken press. The simulation model setup, depicted in figure 5, consists of two rigid shell bodies and the hat profile with a solid mesh model. The total amount of elements is 205500 where 3 elements through thickness are aimed. The nominal element edge length is $1\,mm$. A fully integrated solid element formulation, ELFORM = -1, is used. To prevent self-penetration, the contact definition ***CONTACT_ERODING_NODES_TO_SURFACE** is applied to the hat profile. The crushing load is applied on the top rigid shell body by ***BOUNDARY_PRESCRIBED_MOTION_RIGID** and ***DEFINE_CURVE_SMOOTH.** This explicit simulation is performed with parallel computing on 64 cores in approximately 9 hours.

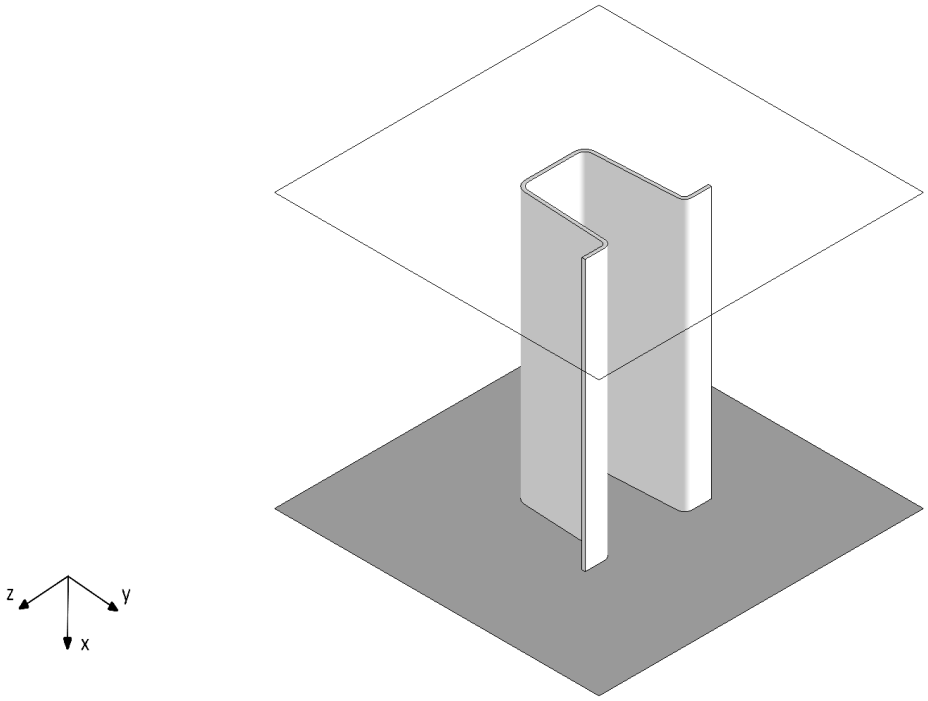

Fig. 5: Simulation setup of the validation test; rigid bodies on the cross sections for the application the crushing load and the hat profile as solid body.

The visual comparison of experiment and simulation is depicted in Figure 6. A well predicted accordance of the deformation behaviour is observed in simulation. Furthermore, the damage incidence during the crushing process is captured in an appropriate manner. In addition, the force-displacement curve of the crushing test is taken into account for the validation of the Wilkins Damage Model. Figure 7 illustrates experimental curves, reduced to the upper and lower deviation bounds, black dashed lines, and two simulation curves, violet and black solid line. The total number of experiments is six. For the evaluation of damage influence in this simulation, an additional simulation with pure elasto-plastic material behaviour without material damage is performed. Figure 7 shows, that force-displacement behaviour until the elastic collapse is captured with both simulations. Furthermore, the decrease after the elastic deformation is predicted in an acceptable manner in both simulations. Obviously, further displacement leads to material failure, because the simulation curves diverges from each other. It is apparent from figure 7 that a simulation without the consideration of material damage leads to a significantly higher force level. The force-displacement curve of the Wilkins Damage Model moves within the experimental deviation bounds until a displacement of approximately $90\,mm$. Further experimental displacements appears in a significant increasing deviation.

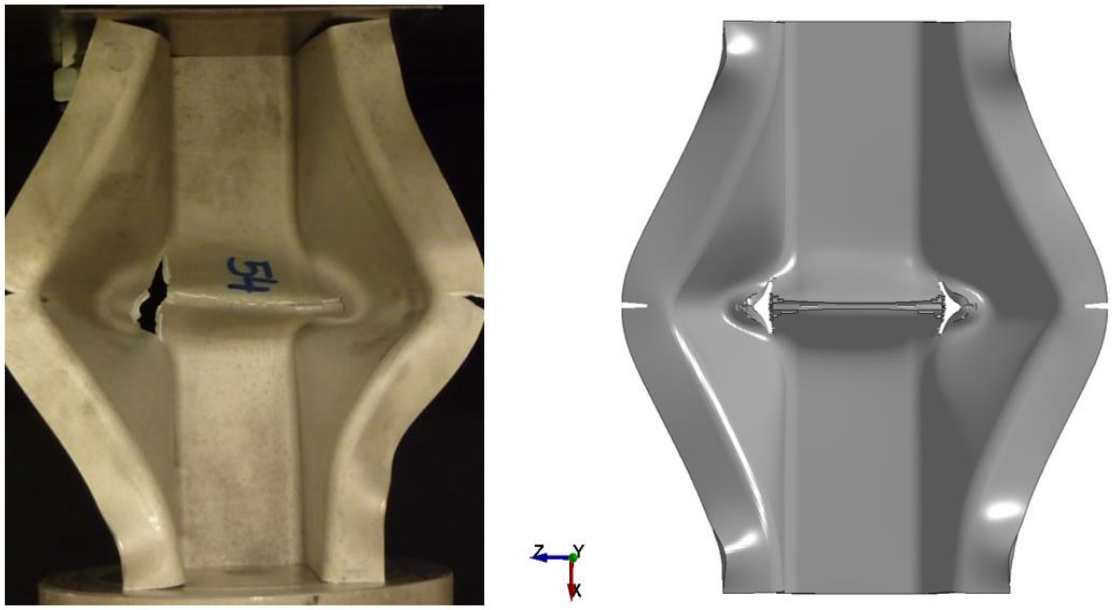

Fig. 6: Experimental result of hat profiles (total length, x: 250 mm, width, z: 117 mm and depth, y: 91 mm) with a subjected crushing displacement of 30 mm (left) and the corresponding simulation in application of the Wilkins Damage Model (right)

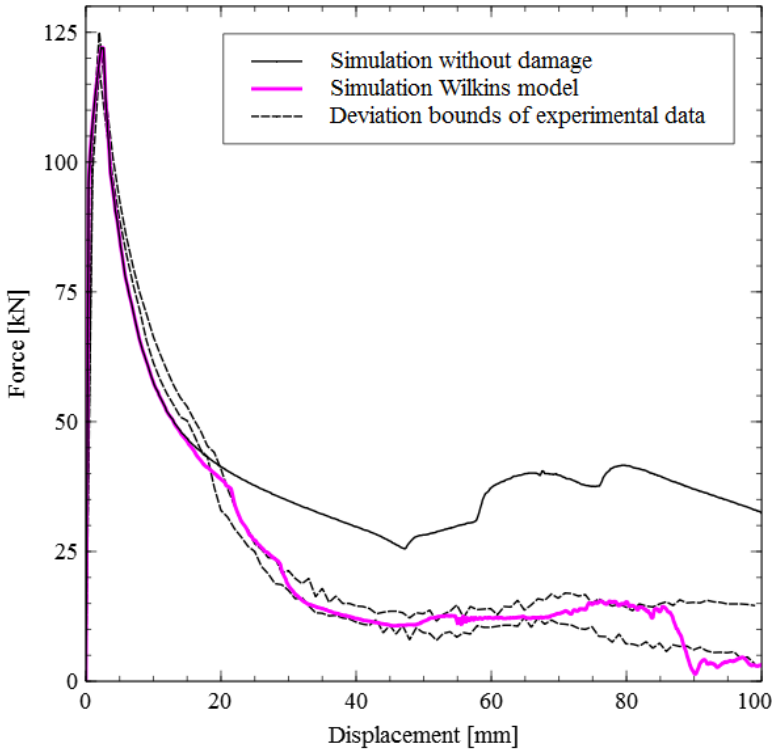

Fig. 7: Experimental and simulation force versus displacement curves of the validation test

The deviations of both simulations compared to the experimental meanvalue, derived by the data of figure 7, are depicted in Table 1. The magnitude of the force peak is captured by both material models equally, because the constitutive formulation is identical in both simulations.

The comparison of total energy absorption values shows a deviation of only 3.63 % of the numerical model to the experimental meanvalue.

Validation parameter	Elasto-plastic + Wilkins Damage Model	Elasto-plastic
Force peak [%]	-0.66	-0.66
Absorbed energy [%]	-3.63	+66.94

*Table 1: Comparison of a pure elasto-plastic material model without damage (***MAT_024**) and the approach of Wilkins (***MAT_082**) in crushing of hat profiles*

7 Summary

The intention of this paper is the investigation on a Material Damage Model introduced by Wilkins by an alternative approach to GISSMO with less calibration effort. The approach of Wilkins for ductile damage proposes damage accumulation due to hydrostatic stress and deviatoric stress combined by plastic strain. The model is calibrated for an AlSi10 cast alloy by different test coupons for various triaxiality regimes. After model calibration, a 3D validation simulation is performed through crushing of a hat profile. The evaluation of this test shows a well accordance of simulation results with respect to experimental tests.

8 Acknowledgement

This work has been supported by the European Regional Development Fund (EFRE) in the framework of the EU-program "IWB Investition in Wachstum und Beschäftigung Österreich 2014-2020", and the federal state Upper Austria.

9 References

[1] Gurson A. L., “Porous rigid-plastic materials containing rigid inclusions-yield function, plastic potential and void nucleation,” The Physical Metallurgy of Fracture, 1978.

[2] Tvergaard, V.; Needleman, A., “An analysis of ductile rupture in notched bars,” Journal of the Mechanics and Physics of Solids, 1984.

[3] Hutchinson, J.; Nahshon, K., “Modification of the Gurson Model for shear failure,” European Journal of Mechanics and Solids 27, 2008, 1-17.

[4] Johnson, G. R.; Cook, W. H., “Fracture characteristics of three metals subjected to various strains, strain rates, terperatures and pressures,” Engineering Fracture Mechanics, 1985, pp. 31–48.

[5] Corporation Livermore Software Technology; (LSTC), “LS-Dyna Keyword User's manual Volume 2 Material models R 7.1,” 2014.

[6] Wilkins, M. L.; Streit, R. D.; Reaugh, J. E., “Cumulative-strain-damage model of ductile fracture: Simulation and prediction of engineering fracture tests,” 1980.

[7] Feucht, M.; Haufe, A.; Andrade, F., “Damage and Failure Models in LS-Dyna,” Dynamore GmbH, Seminarunterlagen, 2016.

[8] Bao, Y.; Wierzbiecki, T., “On the cut-off value of negative triaxiality for fracture,” Engineering Fracture Mechanics, 2005, 72(7):1049 - 1069.

[9] Barsoum, I.; Faleskog, J., “Rupture mechanisms in combined tension and shear-experiments,” International Journal of Solids and Structures, 44(6):1768 - 1786, 2007 .

[10] Hutchinson, J.; Nahshon, K., “Modification of the Gurson Model for shear failure,” European Journal of Mechanics and Solids 27, 2008, 1-17.

[11] Yin, Q.; Zillmann, B.;Suttner S.; Gerstein G.; Biasutti, M.; Tekkaya A.; Wagner M.; Merklein, M.; Schaper, M.; Halle, T.;Brosius,A., “An experimental and numerical investigation of different shear test configurations for sheet metal characterization,” International Journal of Solids and Structures, 2014, pp. 1066-1074.

[12] Tvergaard, V.; Needleman, A., “An analysis of ductile rupture in notched bars,” Journal of the Mechanics and Physics of Solids, 1984.